



## Aerodynamic noise produced in flow around an automobile bonnet

Hiroshi Yokoyama<sup>1</sup>, Takahiro Nakajima<sup>2</sup>, Taishi Shinohara<sup>3</sup>, Masashi Miyazawa<sup>4</sup> and Akiyoshi Iida<sup>5</sup>

<sup>1,2,3,5</sup> Department of Mechanical Engineering, Toyohashi University of Technology

1-1, Hibarigaoka, Tempaku, Toyohashi-shi, Aichi 441-8580, Japan

<sup>4</sup> Department 3, Technology development division 10 Honda R&D Co., Ltd. Automobile R&D Center

4630, Oaza Shimo-Takanezawa, Haga-machi, Haga-gun, Tochigi 321-3393, Japan

### ABSTRACT

To clarify the mechanism and conditions of the intense acoustic radiation from flows around a curvilinear body with a kink shape in an accelerated boundary layer, the experiments were performed with a low noise wind tunnel. The effects of the free-stream velocity and angle of the model to the horizontal surface in the downstream of the kink,  $\gamma$ , on the sound and flow fields were investigated. Consequently, the intense tones can be observed at  $\gamma = 5^\circ, 10^\circ$ . In these cases, the velocity fluctuations showed that the periodic vortex formations occur with the flow separation due to the kink. Also, it was clarified that the fundamental frequency of the tones has ladder-type behavior with reference to the flow velocity. These results indicated that the feedback loop, which consists of the vortex formation due to the kink and acoustic radiation around the trailing edge, is formed. Meanwhile, the intense tones did not radiate for the larger angle of  $\gamma = 15^\circ$ , where the vortex formation does not occur around the kink shape by the lack of flow separation. Also, for the smaller angle of  $\gamma = 0^\circ$ , the large flow separation prompted turbulent transition and the intense tones do not radiate.

Keywords: Flow noise, Trailing edge noise, Automotive Noise  
I-INCE Classification of Subjects Number(s): 21.6

### 1. INTRODUCTION

In recent years, as the reduction of engine noise and road noise has been advanced, the reduction of aerodynamic noise has become one of the most important issues in the development of various high-speed transports such as automobiles. In the case of automobiles, intense tonal sound is often generated from rearview mirrors, front pillars and sunroofs [1, 2]. The mechanism and conditions for tonal sound radiating from the flows over open cavity such as the sunroof has been investigated by a number of authors [3-5]. As a result, flow-acoustic interactions have been clarified to cause the cavity tone. Also, intense tonal sound often radiates from flows around a trailing edge with an upstream kink shape in an accelerated boundary layer as shown in Figure 1. These configurations can be found in automobiles (for example bonnet). However, the radiation mechanism of this sound has not been clarified.

The objective of this investigation is to clarify the mechanism and condition for the radiation of these tones. We performed wind tunnel experiments with kink shape model and measured the sound pressure level and flow fields. The effects of the angle of the model in the downstream of the kink to the horizontal line,  $\gamma$ , and the free stream velocity,  $U_{ref}$ , on the flow and acoustic fields are focused on to understand the generation mechanism of this tonal sound.

---

<sup>1</sup> h-yokoyama@me.tut.ac.jp

<sup>2</sup> nakajima@aero.me.tut.ac.jp

<sup>3</sup> shinohara@aero.me.tut.ac.jp

<sup>4</sup> Masashi\_Miyazawa@n.t.rd.honda.co.jp

<sup>5</sup> iida@me.tut.ac.jp

## 2. METHODOLOGY

### 2.1 Experimental setup

Figure 1 shows in the schematics of experimental setup. The experiments were performed by using a low noise wind tunnel that has an open test section with a square section of 300 mm × 300 mm. Table 1 shows the experimental parameters. In order to keep the two-dimensionality of flow in the span-wise direction, the test section is terminated by two end plates. One of the end plates was made of a porous plate in order to suppress sound reflections and span-wise acoustic resonance. This wind tunnel has a turbulence intensity of less than 0.5 % and non-uniformity of the mean free-stream velocity of less than 0.5 % , and the background noise level of the wind tunnel is 65.2 dB (A) at the flow velocity of 30 m/s.

The model as shown in Figure 1 was used. This model simulates the curvature of an actual automobile bonnet with a kink shape. The origin of the coordinate system was located at the kink. The axis of  $x_d$  was defined in the direction from kink shape to the trailing edge and the axis of  $y_d$  was perpendicular to the axis of  $x_d$ . The angle of  $\beta$  is that formed by the horizontal line and the tangential line of the upstream curve of model at the kink. In this experiment, the angle of  $\beta$  was constant ( $\beta = 16^\circ$ ). The distance from the kink to the trailing edge is  $d = 30$  mm. The reference velocity was measured at 20 mm from the kink shape, and changed from 15 m/s to 36 m/s.

The sound pressure was measured at 800 mm from the kink shape with a non-directional 1/2 inch microphone. The velocity distributions were measured with the hot-wire anemometer.

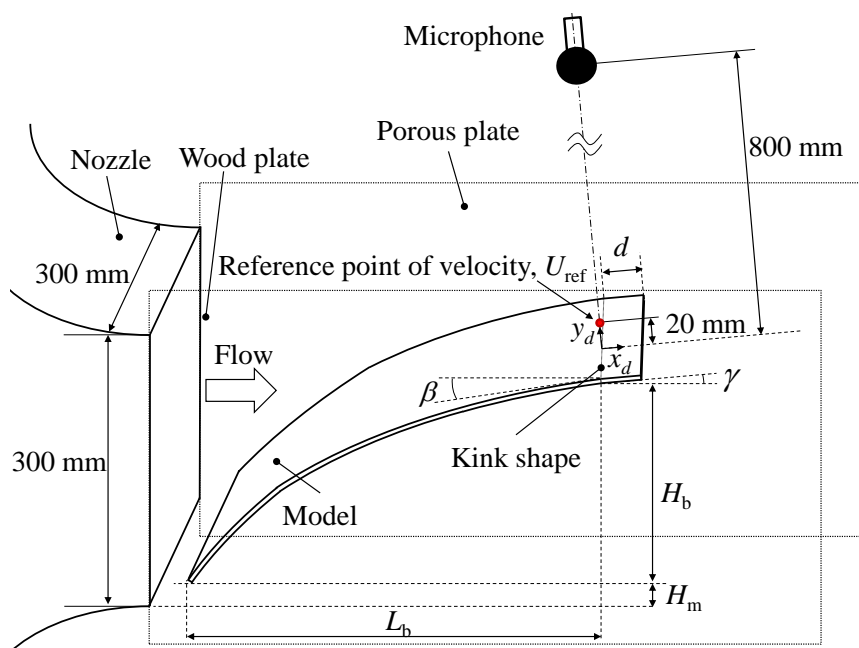


Figure 1 - Schematics of experimental setup

Table 1 - Experimental parameters

$\beta$ [°]	$\gamma$ [°]	$d$ [m]	$U_{ref}$ [m/s]	$M_{ref}$	$Re_d$	$L_b/d$	$H_b/d$	$H_m/d$
16	0, 5, 10, 15	0.03	15 ~ 36	0.044 ~ 0.105	$3.0 \times 10^5 \sim 7.1 \times 10^5$	11	5.13	1.33

### 2.2 Experimental condition

To clarify the effects of the shape of the kink and the free-stream velocity on the tonal sound, the sound pressure level were performed at the 4 angles of  $\gamma = 0^\circ, 5^\circ, 10^\circ, 15^\circ$  and the velocity of  $U_{ref} = 15 \sim 36$  m/s. Table 2 shows in the measuring conditions of the sound pressures. Table 3 shows in the

analysis conditions of the sound pressure spectra. To investigate the effects of the angle on the flow field around the kink shape, the velocity distributions were measured with the hot-wire anemometer for  $\gamma = 0^\circ, 5^\circ, 10^\circ, 15^\circ$  at  $U_{\text{ref}} = 30$  m/s.

Table 2 - Measuring conditions of sound pressure

$\gamma$ [°]	$U_{\text{ref}}$ [m/s]	Sampling frequency [kHz]	Duration time of sampling [s]
0, 5, 10, 15	15 ~ 36	80	30

Table 3 - Analysis conditions of sound pressure spectra

Frequency range [kHz]	Frequency resolution [Hz]	Averaging number
0 ~ 40	9.77	1168

The path for the measurement with the hot-wire anemometer is shown in Figure 2. The stream-wise position for the measurement was  $x_d/d = 0.00, 0.25, 0.50, 0.75, 1.00, 1.17$  and the vertical range was  $0 \text{ mm} \leq y_d \leq 20 \text{ mm}$  ( $x_d/d = 0.00, 0.25, 0.50, 0.75, 1.00$ ) and  $-20 \text{ mm} \leq y_d \leq 20 \text{ mm}$  ( $x_d/d = 1.17$ ). Table 4 shows the measuring conditions of the flow fields, and Table 5 shows the analysis conditions of the power spectra of the velocity fluctuations. The turbulent intensity was computed by integrating the power spectra in the range of 100 Hz ~ 15 kHz to minimize the noises of measurements.

Table 4 - Measuring conditions of flow fields

$\gamma$ [°]	$U_{\text{ref}}$ [m/s]	Sampling frequency [kHz]	Duration time of sampling [s]
0, 5, 10, 15	30	160	30

Table 5 - Analysis conditions of power spectra of velocity fluctuations

Frequency range [kHz]	Frequency resolution [Hz]	Averaging number
0 ~ 80	9.77	1168

The hot-wire anemometer was calibrated by the empirical formula (1). The calibration of the hot-wire anemometer was performed by using the velocity measured by a pitot tube, and the coefficients,  $a$ ,  $b$ , and  $c$  in formula (1) were determined by the least-square method. Table 6 shows the conditions for the calibration of the hot-wire anemometer. After the calibration, the error of the velocity measured by the hot-wire anemometer was as to be within 2 %. An example of the coefficients,  $a$ ,  $b$ , and  $c$  is shown in formula (2).

Table 6 – Calibration conditions of hot-wire anemometer

Sampling frequency [kHz]	Duration time of sampling [s]	$U_{\text{ref}}$ of calibration point [m/s]
20	30	0.5, 3, 6, 10, 15, 22, 30, 33

$$U = (aE^4 + bE^2 + c)^{1/0.45} \quad (1)$$

$$a = -1.2730, b = 0.0504, c = 0.0001 \quad (2)$$

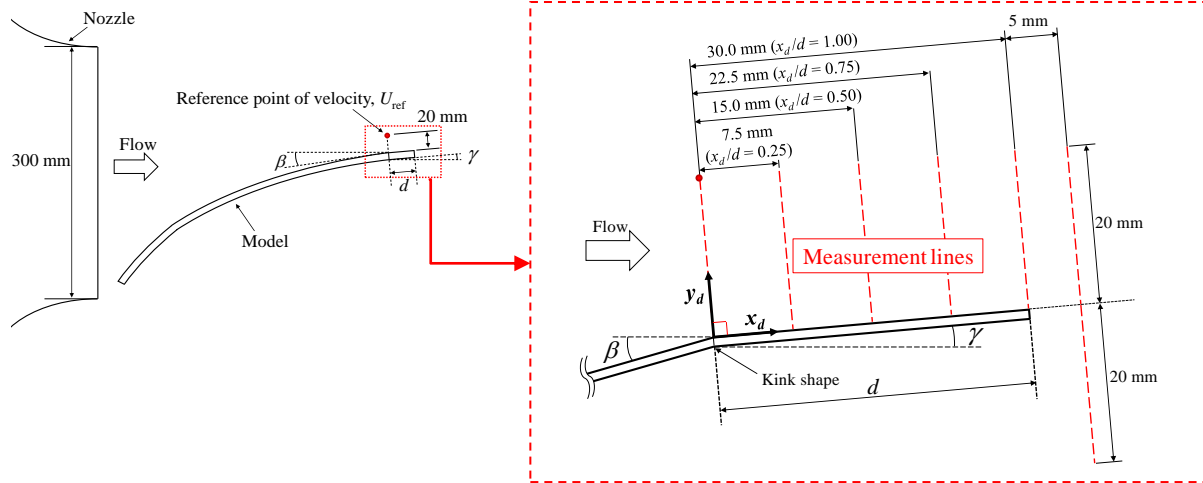


Figure 2 – Measurement lines of flow fields with hot-wire anemometer

### 3. RESULTS AND DISCUSSION

#### 3.1 Aerodynamic Noise around the bonnet model

Figure 3 shows the sound pressure spectra at  $M_{ref} = 0.087$  ( $U_{ref} = 30$  m/s). It was clarified that the tonal sound becomes intense for  $\gamma = 5^\circ, 10^\circ$ . The maximum noise level of 58 dB was observed at  $St = 3.0$  (3.0 kHz) for  $\gamma = 5^\circ$  and the maximum noise level of 50 dB was observed at  $St \equiv fd/U_{ref} = 1.5$  (1.5 kHz) for  $\gamma = 10^\circ$ . Figure 4 shows the dependency of the peak sound pressure level on the free-stream Mach number,  $M_{ref}$ , for  $\gamma = 5^\circ, 10^\circ$ . The tonal sound level increases along with  $M_{ref}$  for  $\gamma = 10^\circ$ , and the maximum noise level of 77 dB was observed at  $St = 1.5$  (1.7 kHz) for  $M_{ref} = 0.104$  ( $U_{ref} = 36$  m/s). Meanwhile, the tonal sound level gradually decreases for  $\gamma = 5^\circ$ . This is possibly because the flow separation in the downstream of the kink is larger and the flow around the kink shape becomes turbulent as the velocity increases. The maximum noise level of 63 dB was observed at  $St = 2.0$  (1.7 kHz) at  $M_{ref} = 0.076$  ( $U_{ref} = 26$  m/s) for  $\gamma = 5^\circ$ .

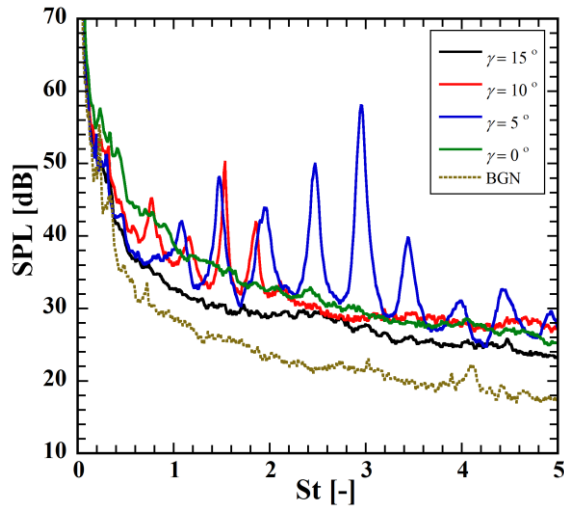


Figure 3 - Effect of angle of  $\gamma$  on sound pressure spectra at  $M_{ref} = 0.087$  ( $U_{ref} = 30$  m/s)

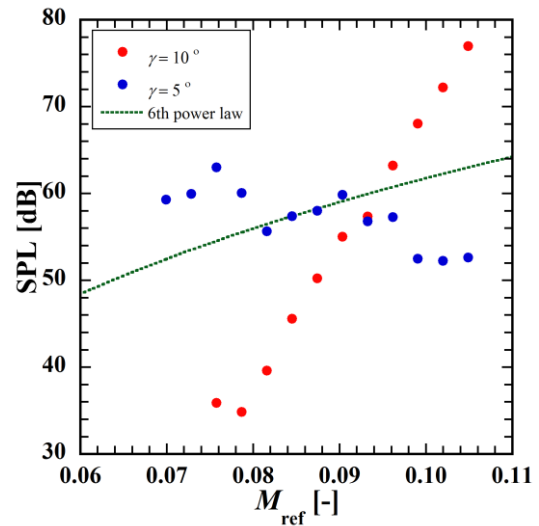


Figure 4 - Dependency of peak sound pressure level on freestream Mach number.

Figures 5 and 6 show the effects of  $M_{ref}$  on Strouhal number for  $\gamma = 5^\circ, 10^\circ$ , respectively. The dominant peak frequency jumps from  $St = 2.5$  to  $St = 3.0$  at  $M_{ref} = 0.082$  ( $U_{ref} = 28$  m/s) for  $\gamma = 5^\circ$ . This ladder-type behavior was also observed in flows around an airfoil in the past research [6-8].

This indicates that the acoustic-fluid interactions occur in the present configurations like in flows around an airfoil. These interactions have been confirmed to occur by the direct numerical simulations [9].

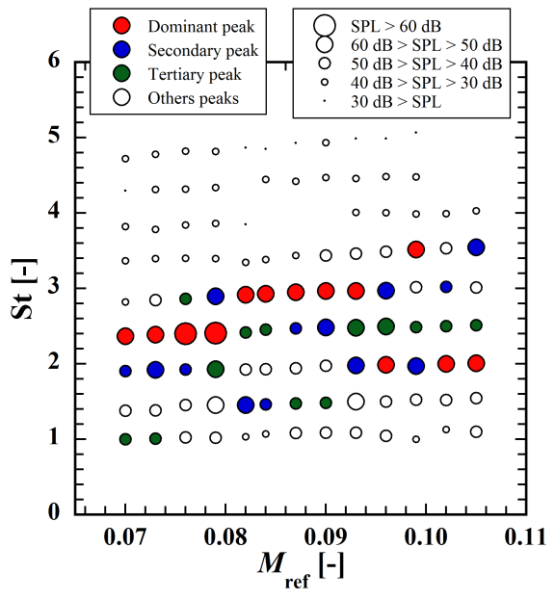


Figure 5 - Effects of the free-stream Mach number,  $M_{ref}$ , on Strouhal number ( $\gamma = 5^\circ$ )

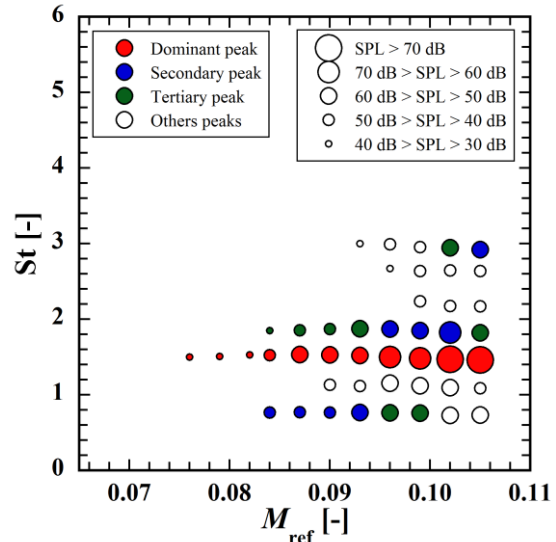


Figure 6 - Effects of the free-stream Mach number,  $M_{ref}$ , on Strouhal number ( $\gamma = 10^\circ$ )

### 3.2 Flow field around kink shape

#### 3.2.1 Flow field for intense acoustic radiation ( $\gamma = 5^\circ, 10^\circ$ )

Figure 7 shows the profile of the mean velocity for  $\gamma = 0^\circ, 5^\circ, 10^\circ, 15^\circ$  at  $M_{ref} = 0.087$  ( $U_{ref} = 30$  m/s). Under the condition for the radiation of the intense tonal sound ( $\gamma = 5^\circ, 10^\circ$ ), the separation was observed at  $x_d/d = 0.25, 0.50$  for  $\gamma = 5^\circ, 10^\circ$ , respectively. Also, the reattachment was observed at  $x_d/d = 0.75$  for  $\gamma = 5^\circ$ , where the most intense sound radiates at this Mach number. Figure 7 also shows the profile of the intensity of turbulence. The height of the peaks of these profiles is approximately corresponding to that of the high shear rate of the mean profile.

Figure 8 shows the power spectra of the velocity fluctuations at  $x_d/d = 0.50, 1.00$  for  $\gamma = 0^\circ, 5^\circ, 10^\circ, 15^\circ$  at  $M_{ref} = 0.087$  ( $U_{ref} = 30$  m/s). Figure 9 and 10 shows the comparison of the power spectra of the velocity fluctuations and the sound pressure spectra for  $\gamma = 5^\circ, 10^\circ$ , respectively. Under the condition for the intense acoustic radiation ( $\gamma = 5^\circ, 10^\circ$ ), the peaks are observed in the spectra. The frequencies of peak are  $St = 2.5, 3.0, 3.5$  (2.5 kHz, 3.0 kHz, 3.5 kHz) for  $\gamma = 5^\circ$ . The frequencies of peak are  $St = 1.5, 1.8$  (1.5 kHz, 1.8 kHz) for  $\gamma = 10^\circ$ . These peak frequencies are the same as those of the sound pressure spectra. These indicate that the periodic vortex formation occurs between the kink and the trailing edge. As the vortex passes the trailing edge, the deformation of the vortex occurs and cause intense tonal sound.

#### 3.2.2 Flow field for weak acoustic radiation ( $\gamma = 0^\circ, 15^\circ$ )

Figure 7 shows that the flow separation does not occur for  $\gamma = 15^\circ$ . Figure 8 also shows that the power spectra have no peak. For this angle, the periodic vortex formation does not occur by the lack of the flow separation.

For  $\gamma = 0^\circ$ , the flow separation is very large as shown in Figure 7. However, the periodic vortex formation does not occur as shown in Figure 8. This is because the turbulent transition of the flow in the downstream of the kink is prompted due to the large separation. Figure 8 shows that the curve of the spectrum is along the slope of the power of  $-5/3$  at  $St = 3$  for  $\gamma = 0^\circ$ , while the spectrum for  $\gamma = 5^\circ$  has intense peak around that frequency. This indicates that the flow becomes turbulent for  $\gamma = 0^\circ$ . As a result, the span-wise phase of the vortices is not coherent and the intense tonal sound does not radiate.

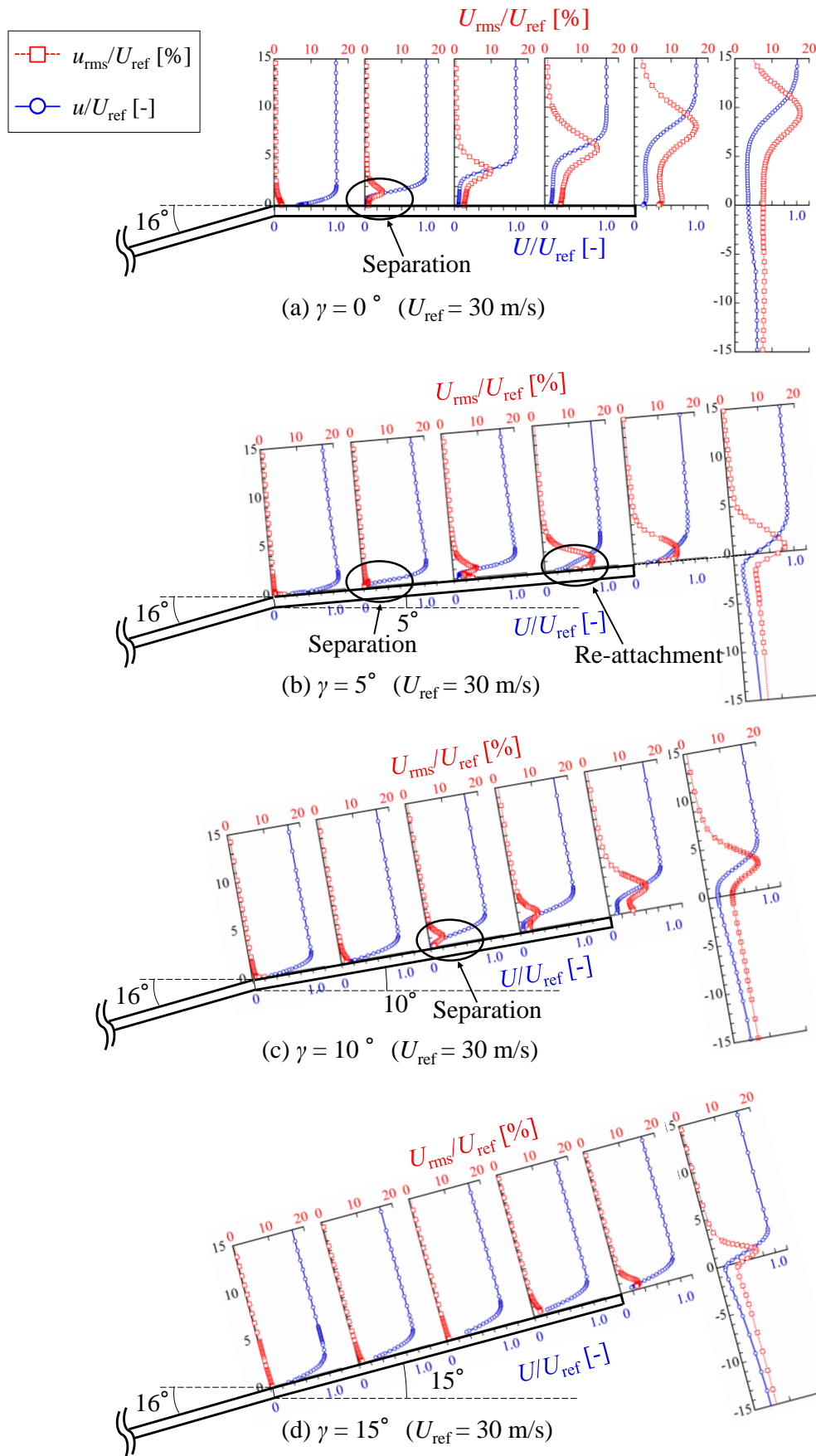


Figure 7 – Effects of angle of  $\gamma$  on flow field ( $\gamma = 0^\circ, 5^\circ, 10^\circ, 15^\circ, U_{ref} = 30$  m/s)

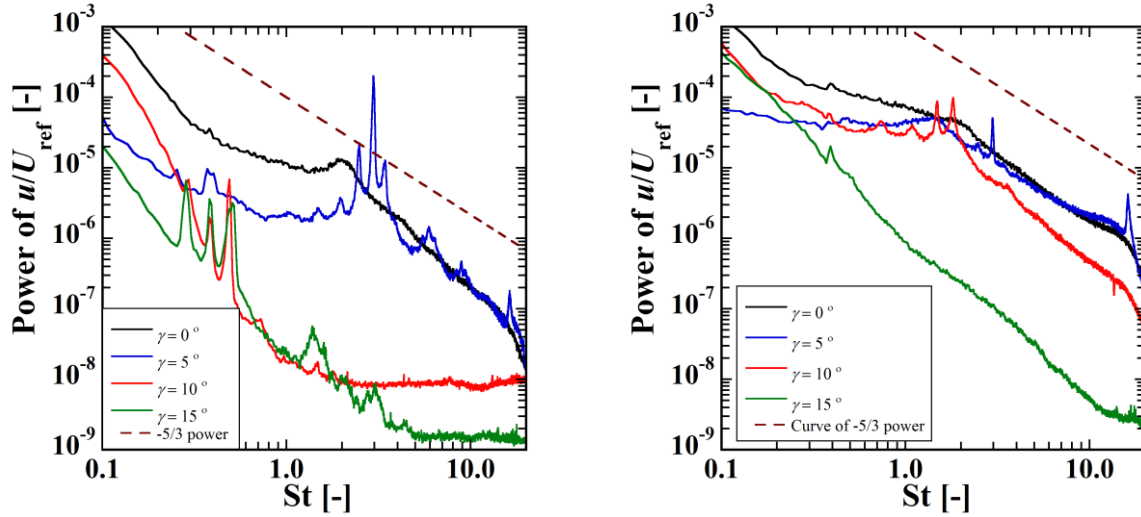


Figure 8 - Effect of angle of  $\gamma$  on velocity fluctuation spectra at  $x_d/d = 0.5$  (left) and  $1.0$  (right)  
 ( $U_{ref} = 30$  m/s)

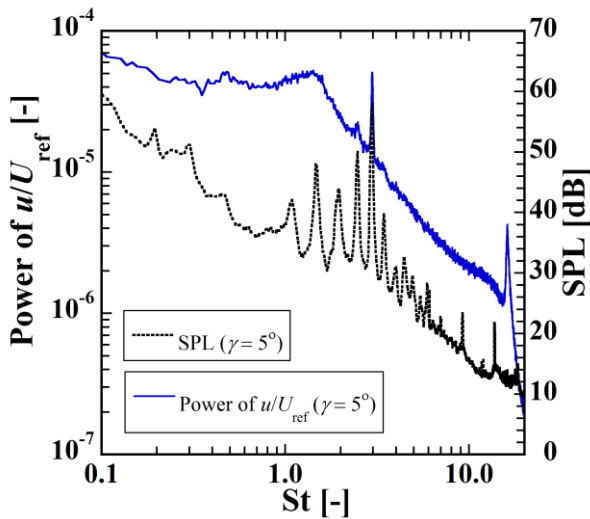


Figure 9 – Comparison of power spectrum of velocity fluctuations and sound pressure spectrum  
 ( $\gamma = 5^\circ$ ,  $U_{ref} = 30$  m/s,  $x_d/d = 1.00$ )

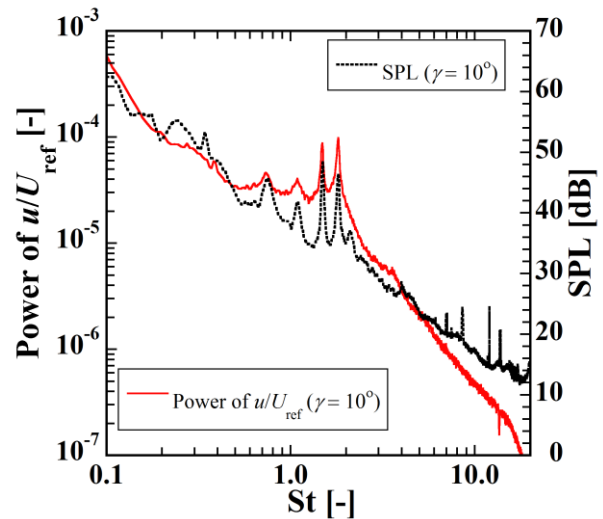


Figure 10 - Comparison of power spectrum of velocity fluctuations and sound pressure spectrum  
 ( $\gamma = 10^\circ$ ,  $U_{ref} = 30$  m/s,  $x_d/d = 1.00$ )

#### 4. CONCLUSIONS

In order to clarify the mechanism and the condition of the radiation of intense tones radiating from a flow around a curvilinear body with a kink shape in an accelerated boundary layer, the sound pressure level and flow fields were measured at the angle of model to the horizontal surface,  $\gamma = 0, 5, 10, 15^\circ$ , and  $M_{ref} = 0.044 \sim 0.105$  by using a low noise wind tunnel.

As a result, it was clarified that intense tone is observed for  $\gamma = 5^\circ$  at  $M_{ref} = 0.076 \sim 0.105$  ( $U_{ref} = 26 \sim 36$  m/s) and  $\gamma = 11^\circ$  at  $M_{ref} = 0.070 \sim 0.105$  ( $U_{ref} = 24 \sim 36$  m/s). In addition, the intense tone has ladder-type structure with reference to the free-stream Mach number. This indicates that the acoustic-fluid interactions occur in the present configurations like in flows around an airfoil. The measurement of the flow fields presented that the flow separation occurs for  $\gamma = 5^\circ, 10^\circ$  and the flow re-attachment occurs only for  $\gamma = 5^\circ$ . In addition, the power spectra of the velocity fluctuations showed the peaks and this indicates that the periodic vortex formation occurs between the kink shape and the trailing edge of the model. These peak frequencies of velocity fluctuations coincide with the

peak frequencies of sound pressure level. As the vortex passes a trailing edge, the deformation of the vortex occurs and causes the intense tone.

In contrast, intense tone was not observed for  $\gamma = 0^\circ, 15^\circ$ . The flow separation does not occur between the kink and the trailing edge for  $\gamma = 15^\circ$ . As a result, the vortex formation as described above does not occur and the intense tonal sound does not radiate. Meanwhile, for  $\gamma = 0^\circ$ , the turbulent transition of the flow is prompted by the large separation. As a result, the span-wise phase of the vortices is not coherent, and intense tone does not occur.

## ACKNOWLEDGEMENTS

The present study was supported by JSPS KAKENHI Grant of No. 24760134, that of No. 26820044 and through the Next-generation Supercomputer Strategy Program by the Ministry of Education, Culture, Sports, Science, and Technology of Japan (MEXT).

## REFERENCES

- [1] Li Y, Kamioka T, Nouzawa T, Nakamura T, Okada Y, Ichikawa, N. Evaluation of Aerodynamic Noise Generated in Production Vehicle Using Experiment and Numerical Simulation. SAE Paper 2003; 2003-01-1314.
- [2] Alam F, Watkins S, Zimmer G, Humphris C. Effects of Vehicle A-pillar Shape on Local Mean and Time-Varying Flow Properties. Society of Automotive Engineers 2001; 2001-01-1086.
- [3] Rockwell, D. Naudascher, E. Review-self-sustaining oscillations of flow past cavities. ASME Transactions, Journal of Fluids Engineering Vol. 100; 1978. p. 152-165.
- [4] Rossiter JE. Wind-Tunnel Experiments on the Flow over Rectangular Cavities at Subsonic and Transonic Speeds. Aeronautical Research Council Reports and Memoranda No. 3438; 1964
- [5] Yokoyama H, Kato C. Fluid-acoustic interactions in self-sustained oscillations in turbulent cavity flows, I. Fluid-dynamic oscillations. Physics of Fluids, Vol.21, No.10; 2009. pp. 105103-1-105103-13.
- [6] Paterson RW, Vogt PG, Fink MR. Vortex Noise of Isolated Airfoils. Journal of Aircraft Vol. 10; 1973. p. 296-302.
- [7] Tam CKW. Discrete tones of isolated airfoils. Journal of the Acoustical Society of America Vol.55 No.6; 1974. p. 1173-1177.
- [8] Arbey H, Bataille J. Noise generated by airfoil profiles placed in a uniform laminar flow. Journal of Fluid Mechanics Vol.134; 1983. p. 33-47.
- [9] Yokoyama H, Shinohara T, Miyazawa M, Iida A. Acoustic Radiation in Flows around a Trailing Edge with an Upstream Kink Shape. Proc INTER-NOISE 2013; 15-18 September 2013; Innsbruck, Austria 2013.